SEARCH FOR ANTIMATTER IN SPACE WITH THE ALPHA MAGNETIC SPECTROMETER

R. Battiston
Dipartimento di Fisica and Sezione INFN
Via Pascoli, Perugia, 06100 , Italy
E-mail:battisto@krenet.it
AMS Collaboration

ABSTRACT

The Alpha Magnetic Spectrometer (AMS) is a state of the art particle physics experiment for the extraterrestrial study of antimatter, matter and missing matter. AMS successfully completed the precursor STS91 Discovery flight (June 2nd-12th, 1998), completing 152 orbits at $\pm 52^o$ of latitude and about 400 km of height, collecting more than 100 million CR events. In this paper we report on the first flight experience and we present preliminary results on the search for nuclear antimatter. No antimatter nuclei with $Z \geq 2$ were detected. We obtain a model dependent upper limit on $\Phi_{\bar{H}e}/\Phi_{He}$ of $< 1.14\ 10^{-6}$. In the rigidity region between 1.6 to 20 GV we obtain a model independent, conservative upper limit on $\Phi_{\bar{H}e}/\Phi_{He}$ of $< 1.7\ 10^{-6}$ and of $< 2.8\ 10^{-5}$ for $Z > 2$, improving the results of previous searches performed with stratospheric balloons

Invited talk at XIIIth Rencontres de Physique: Results and Perspectives in Particle Physics, La Thuile, Aosta Valley, February 22-27, 1999.

1 Introduction

The disappearance of cosmological antimatter and the pervasive presence of dark matter are two of the greatest puzzles in the current understanding of our universe.

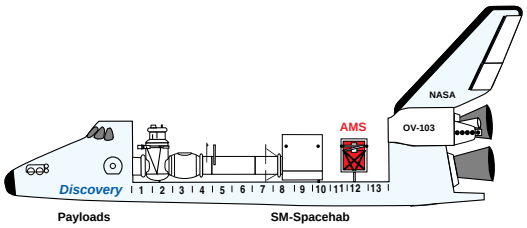

Figure 1: AMS on STS 91 (Discovery), June 2nd - 12th, 1998.

The Big Bang model assumes that, at its very beginning, half of the universe was made out of antimatter. The validity of this model is based on three key experimental observations: the recession of galaxies (Hubble expansion), the highly isotropic cosmic microwave background and the relative abundances of light isotopes. However, a fourth basic observation, the presence of cosmological antimatter somewhere in the universe, is missing. Indeed measurements of the intensity of gamma ray flux in the MeV region exclude the presence of a significant amount of antimatter up to the scale of the local supercluster of galaxies (tens of Megaparsecs). Antimatter should have been destroyed immediately after the Big Bang due to a mechanism creating a matter-antimatter asimmetry through a large violation of CP and the baryon number [1)]. Alternatively matter and antimatter were separated into different region of space, at scales larger than superclusters [2)]. Other possibilities have also been recently suggested [3)]. All efforts to reconcile the the absence of antimatter with cosmological models that do not require new physics failed [4)].

We are currently unable to explain the fate of half of the baryonic matter present at the beginning of our universe.

Rotational velocities in spiral galaxies and dynamical effects in galactic clusters provide us convincing evidence that, either Newton laws break down at scales of galaxies or, more likely, most of our universe consists of non-luminous (dark) matter [5)]. There are several dark matter candidates (for a recent review see [6)]). They are commonly classified as "hot" and "cold" dark matter, depending on their relativistic properties at the time of decoupling from normal matter in the early universe. As an example, light neutrinos are obvious candidates for "hot" dark matter while Weakly Interacting Massive Particles (WIMP's) like the lightest SUSY particle (LSP) are often considered as plausible "cold" dark matter candidate [7)]. Even the recent results suggesting a positive cosmological constant [8)] reducing the amount of matter in the universe, confirm the dominance of dark matter over baryonic matter.

We are then unable to explain the origin of most of the mass of our universe.

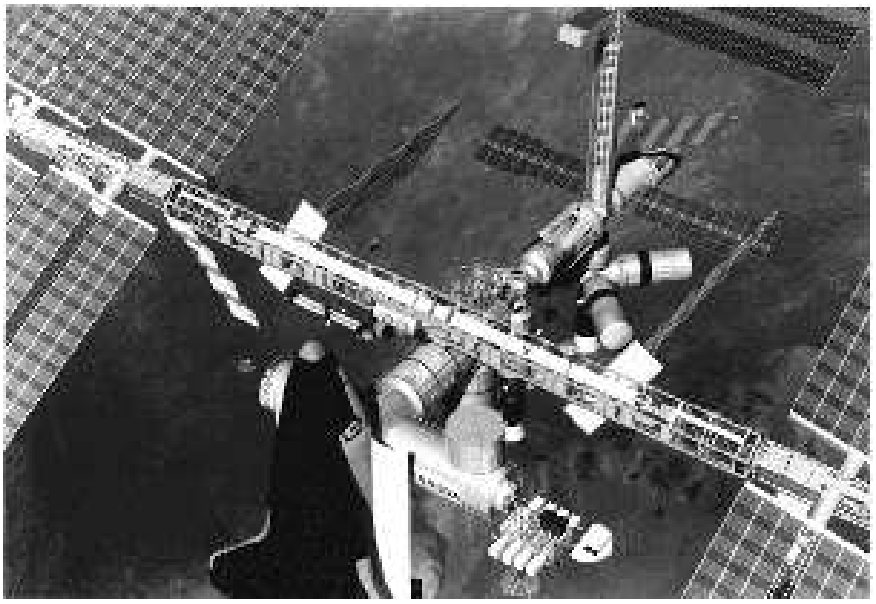

Figure 2: The International Space Station Alpha; AMS will be installed on the left side of the main truss.

To address these two fundamental questions in astroparticle physics a state of the art particle detector, the Alpha Magnetic Spectrometer (AMS) [9] has been approved in 1995 by NASA to operate on the International Space Station (ISS).

AMS has successfully flown on the precursor flight (STS91, Discovery, June 2nd 1998, Figure 1), and it is approved for a three year long exposure on the International Space Station (ISS), (Figure 2), after its installation during Utilization Flight n.4, now scheduled in 2004. AMS has been proposed and has been built by an international collaboration coordinated by DoE, involving China, Finland, France, Germany, Italy, Portugal, Rumenia, Russia, Spain, Switzerland, Taiwan and US.

In this conference we report on the operation of AMS during the precursor flight and we give preliminary results on the search for nuclear antimatter.

2 AMS design principles and operation during the Shuttle flight

Search of antiparticles requires the capability to identify with the highest degree of confidence, the type of particle traversing the experiment by measuring its mass, the absolute value and the sign of its electric charge. This can be achieved through repeated measurements of the particle momentum (Magnetic Spectrometer), velocity (Time of Flight, Cerenkov detectors) and energy deposition (Ionization detectors).

AMS configuration on the precursor flight is shown in Figure 3. It consists on a large acceptance magnetic spectrometer (0.6 m^2sr) based on a permanent Nd-Fe-B Magnet , surrounding a six layer high precision Silicon Tracker and sandwiched

between the four planes of the Time of Flight scintillator system (ToF).

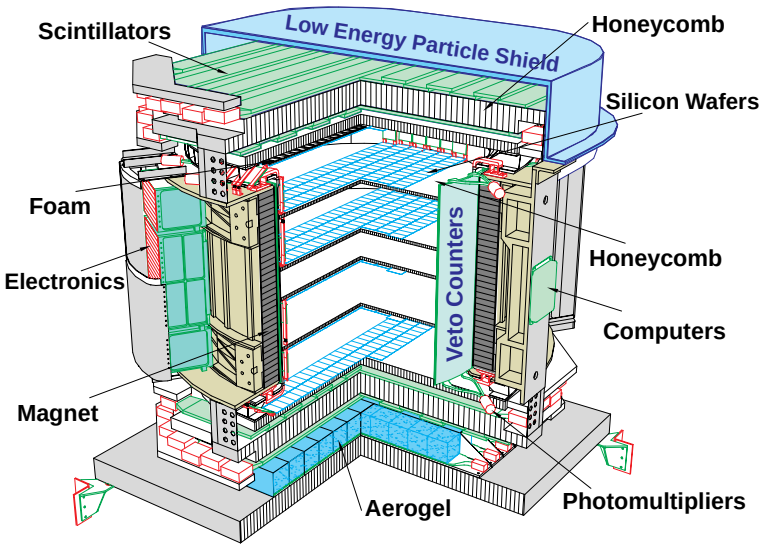

Figure 3: AMS configuration for the June 1998 Shuttle precursor flight (STS91); about 45% of the Silicon Tracker was equipped during this mission.

A scintillator Anticounter system, located on the magnet inner wall and a aerogel threshold Cherenkov detector ($n = 1.035$), complete the experiment. A thin shield on the top and the bottom sides absorb low energy particles present on the Earth radiation belts. The detector works in vacuum: the amount of material in front of the ToF is about 1.5 g/cm^2 and 4 g/cm^2 in front of the Tracker.

The magnet is based on recent advancements in permanent magnetic material technology which made it possible to use very high grade Nd-Fe-B to construct a permanent magnet with $BL^2 = 0.15\ Tm^2$ weighting ≤ 2 tons. The magnet has a cylindrical shape with 80 cm of height and an internal diameter of 100 cm. A charged particle traversing the spectrometer experiences a dipole field orthogonal to the cylinder axis: it triggers the experiment through the ToF system (planes $S1$ to $S4$) which also measures the particle velocity (β) with a typical resolution of 105 ps over a distance of $\sim$ 1.4 m.

The curvature of the tracks is measured by up to six layers of silicon double sided detectors, supported on ultralight honeycomb planes: the total material traversed by a particle is very small, 3.2% of X_0 over the tracking volume and for normal incidence. The momentum resolution of the Silicon Spectrometer [10] is about 8% in the region between 3 and 10 GV of rigidity: at lower rigidities its resolution worsen due to the multiple scattering while, at high energy, the maximum detectable rigidity ($\frac{\Delta R}{R} = 100\%$) is about 500 GV. The Tracker rigidity resolution function was measured at the GSI ion accelerator facility in Darmstadt in october 1998, using He and C beams, and at CERN in november of the same year, using a proton beam.

The results confirm the design value; an example of the measured resolution is shown in Figure 4. The parameters of the Silicon Spectrometer are given in Table 1: about 45% of the Tracker sensitive area was equipped during the precursor flight, with a corresponding reduction on the spectrometer acceptance.

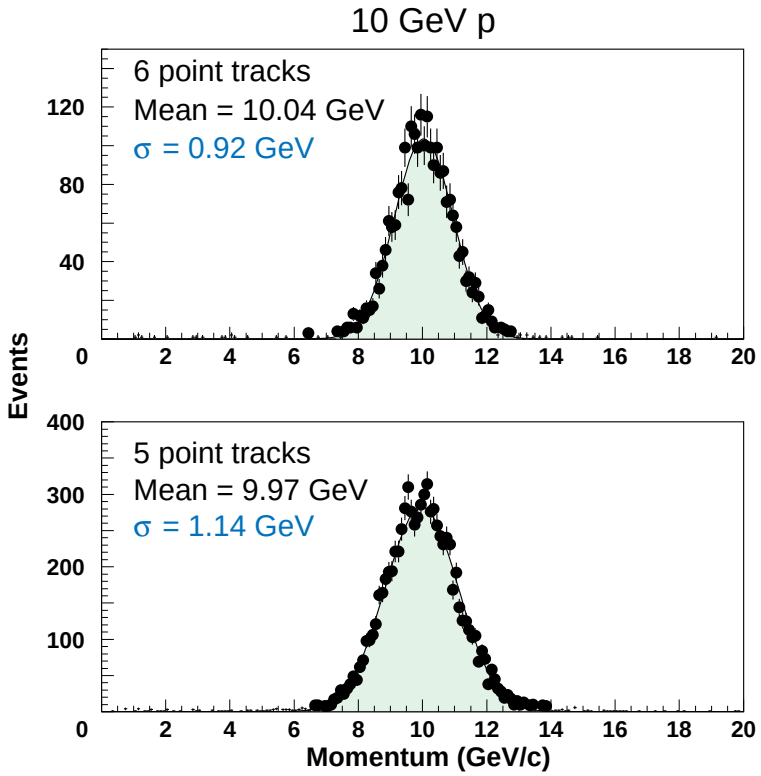

Figure 4: Measurement of the Tracker momentum resolution at 10 GeV using a proton beam at CERN.

Both the ToF scintillators and the Silicon Tracker layers measure $\frac{dE}{dx}$, allowing a multiple determination of the absolute value of the particle charge, Z. Figure 5 show the measurement of the energy deposited by different light nuclei during the precursor flight.

Table 1: AMS silicon Tracker parameters (in parenthesis the values used on the precursor flight).

Number of planes	8
	(6)
Accuracy (bending plane)	10 μm
Accuracy (non bending plane)	30 μm
Number of channels	163936
	(58368)
Power consumption	400 W
	(180 W)
Weight	130 kg
Silicon Area (double sided)	5.4 m^2
	(2.4 m^2)

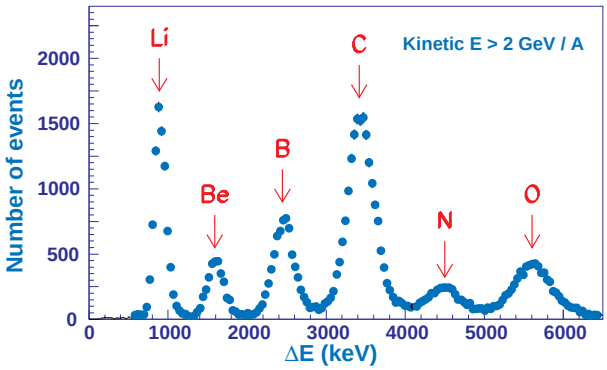

Figure 5: Energy deposition of the light ions as measured by the ToF and Silicon Tracker systems.

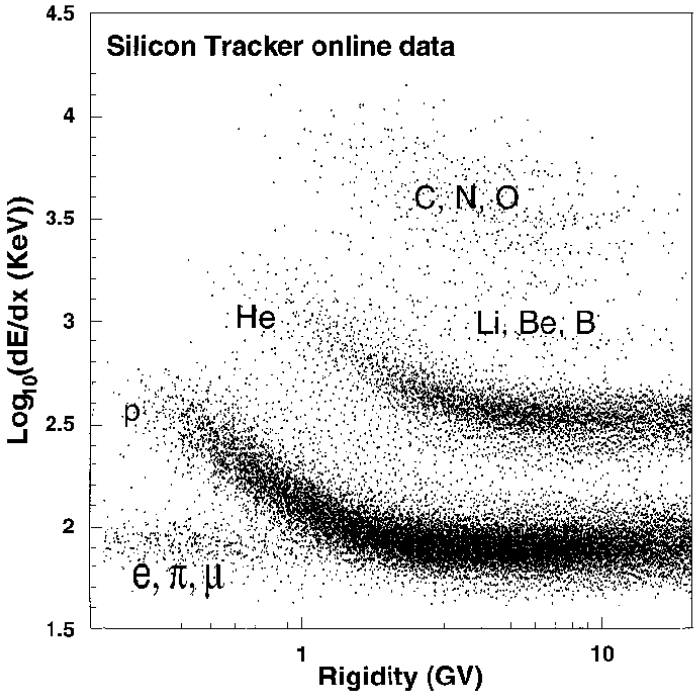

Figure 6: STS91 AMS flight online monitoring data. Both dE/dx and $|R| = |p/Z|$ are measured with the Silicon Tracker.

All detector elements during production have undergone thermo-vacuum tests which have demonstrated that neither the deep vacuum nor important temperature variations deteriorate detector performances. Systematic vibration tests qualified that the mechanical design and workmanship were suited to stand the mechanical stresses during launch and landing.

During the STS91 mission the Spectrometer collected data at trigger rates varying from $\sim 100\ Hz$ at the equator to $\sim 700\ Hz$ at $\pm 52^o$, where the event rate was limited by the data acquisition speed.

After preprocessing and compression, the data were stored on hard disks located on the Shuttle. A total of about 100 million triggers have been recorded during the ten days mission. A considerable part of the time, however, the Shuttle was docked to the MIR station: in this condition the orientation was no good for the AMS since it was sometimes pointing towards Earth. Besides, some element of the station were in the AMS view, thus producing additional unwanted background. The useful time when only deep space was seen by the experiment was about 4 days. Samples of the data ($< 10\%$ of the total) were are also sent to ground in real time using S-band receiving ground stations at an average rate of 1 Mbit/s. Although only rough calibrations were applied to these data, the reconstructed events were used online to monitor AMS operating conditions during the mission.

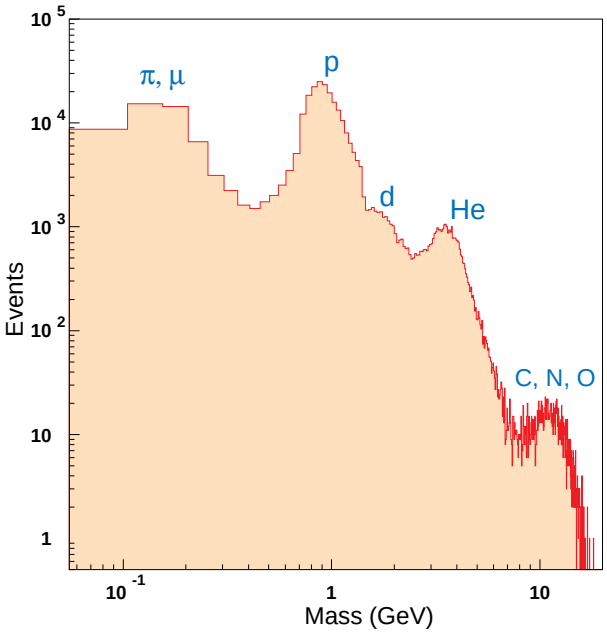

Figure 7: STS91 AMS flight online monitoring data. Mass spectrum obtained by the combined measurement of the Silicon Tracker (R) and the Time of Flight (β).

For example, Figure 6 shows the Tracker response to different types of CR during the MIR docking period: the double logarthmic plot $\frac{dE}{dx}$ versus $|R| = |\frac{p}{Z}|$ clearly shows bands corresponding to light particles ($e^{\pm}, \mu^{\pm}, \pi^{\pm}$), $p^{\pm}$, $^3He/^4He$ and heavier ions. Figure 7 show the CR mass spectrum obtained from R measured by the Tracker and β measured by the ToF.

A candidate $\bar{p}$ event, measured online, is also shown in Figure 8: one can note that the occupancy of the Silicon Tracker is very low, allowing unambiguous reconstruction of the particle trajectory in the magnetic field, meaning the sign of its charge and its momentum.

After landing, the full set of hard disks containing the data has been duplicated and the copy has been transported to CERN. During the month of august we determined the in flight calibration constants for the various detectors. The first mass production took place in the fall of 1999 using a cluster of Alpha stations located at CERN.

3 Antimatter Search

To search for nuclear antimatter, we search for particles with

- negative rigidity;
- module of the charge Z equal or greater than 2;

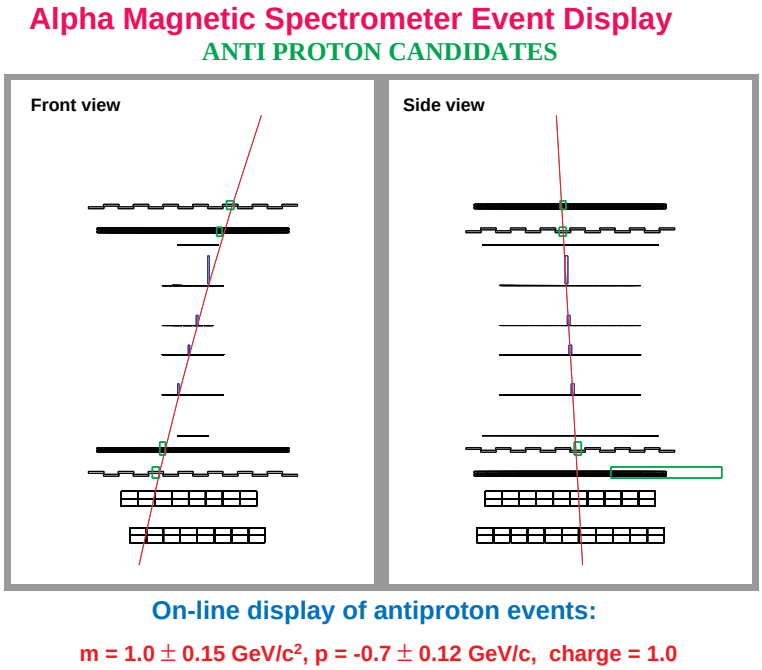

Figure 8: Candidate antiproton event from online monitoring data of the AMS precursor flight. In the front view the fraction of Silicon Tracker equipped during the precursor flight is clearly visible.

- mass equal of greater than the He mass.

These quantities are obtained through repeated measurements of the velocity and its direction (ToF counters), the signed momentum by the Silicon Spectrometer, the absolute value of the charge from $\frac{dE}{dx}$ measurements of up to four ToF layers and up to 6 Silicon Tracker layers.

We start with a preselection of $Z > 1$ particles and apply soft quality cuts to reject background particles with negative momentum ($\bar{He}$ and antinuclei with $Z > 2$ candidates). The effects of these cuts is studied on control samples containing 5.7 M He and 276 K $Z > 2$ events.

- To reject background due to single nuclear scattering in the Tracker we apply cuts on the particle rigidity R. R is measured by the Silicon Spectrometer, using tracks having 5 or 6 points. Since during the precursor flight the Tracker was only partially equipped, we inclued in this analysis also events containing a track detected only on 4 planes.

  The particle rigidity is measured three times: the first two measurements r_1^n and r_2^n are obtained by using three consecutive points out of the total number of measured points n, in the following way: 6 points patterns $r_1^6 = r_{123}$, $r_2^6 = r_{456}$,

5 points patterns $r_1^5 = r_{123}$, $r_2^5 = r_{345}$, 4 points patterns $r_1^4 = r_{123}$, $r_2^4 = r_{234}$, where the lower indices represent the consecutive planes partecipating to the track fit. The third measurement, R, is obtained from a fit of all the points associated with one track. In order to take properly into account the presence of multiple scattering, we used the GEANE fitting procedure [11]. The three determination of the rigidity are compared requiring that they give the same sign of the charge and consistent measurements of the momentum components. In particular, the comparison of the relative rigidity error $\frac{\Delta R}{R}$ with the rigidity asymmetry $A_{12} = (r_1^n - r_2^n)/(r_1^n + r_2^n)$ allows the removal of about 90% of the negative momentum particles while keeping 79% of the He control sample.

- To reject background due to an interaction of the primary particle in the Tracker material we apply cuts on isolation of the clusters detected on the silicon planes. Events where too much energy is observed within 5 mm of the track are rejected. This cut reject fifteen times more particle in the sample with negative momentum: the positive momentum control samples are basically unaffected (97% of the events pass the cuts).

- To separate between upward going and downward going particles we use the ToF measurement.

- The Identification of the absolute value of the particle charge is based on the repeated measurement of the $\frac{dE}{dX}$ on the Silicon Tracker and ToF: we measure a contamination between p and He below the 10^{-7} level.

After the preselection we apply additional χ^2-cuts on the track and ToF measurements and on an overall likelihood function describing the probability of an event to be compatible with He, or heavier nucleus, kinematics, mass and velocity. Some of these cuts are stricter for events hitting only 4 planes. After these cuts all the candidates in the $\bar{He}$ sample were removed while $2,8$ M events on the He sample survived, giving a total efficiency of about 49%. Similarly 156 K events with $Z > 2$ survived the cuts, but none with negative momentum, with a corresponding cuts efficiency of about 56%. The spectra of the positive charge samples after the cuts are shown in Figure 9: the spectra extends above 100 GV of rigidity for both samples. The corresponding Tracker rigidity resolution is shown in Figure 10.

4 Antimatter Limits

To establish a preliminary antimatter upper limit we proceed as follows. The flux of incident He nuclei in a rigidity bin $(r, r + \Delta r)$ as a function of the measured rigidity r, $\Phi_{He}(r)$, is related to the measured He flux, $\Phi_{He}^M(r)$, by

$$\Phi_{He}(r) = \epsilon_{He}^{-1}(r)\Phi_{He}^M(r) \tag{1}$$

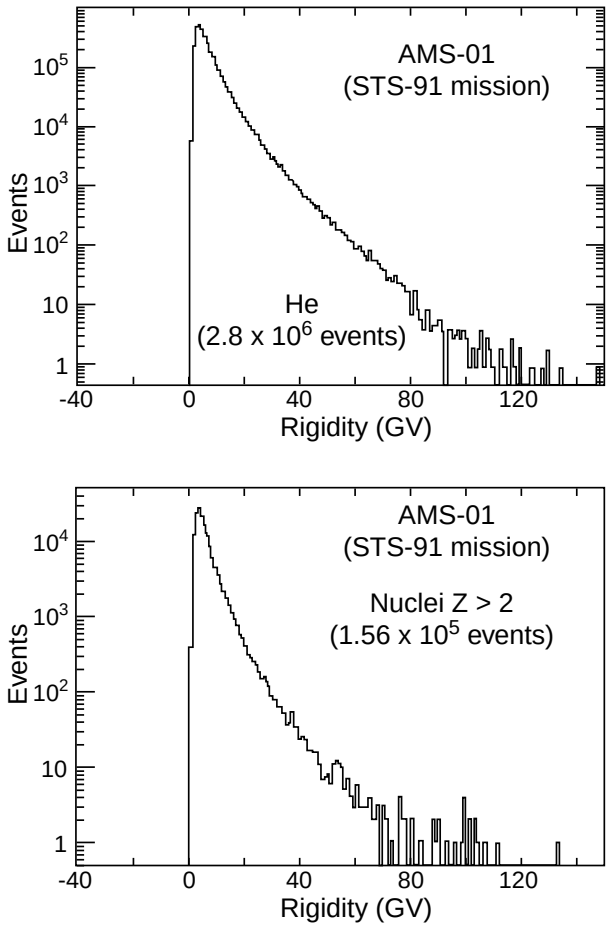

Figure 9: Light nuclei spectra (control samples) as measured in the AMS precursor flight after having applied the antimatter selection cuts discussed in the text.

where $\epsilon_{He}(r)$ is the rigidity dependent selection efficiency of the cuts discussed in the previous section, simulated through a complete MC simulation using the GEANT [11] package. Trigger efficiency and the rigidity dependence of the anticounter veto as well as the corrections due to electronics dead time which was important on polar regions, was checked with events taken with an unbiased trigger. We also corrected $\epsilon_{He}(r)$ for the $He - \bar{He}$ difference in absorption cross sections [12].

Since we detected no $\bar{He}$ candidate, the differential upper limit for the flux ratio at 95% CL is given by:

$$\frac{\Phi_{\bar{He}(r)}}{\Phi_{He}(r)} < \frac{3/\epsilon_{\bar{He}}(r)}{\epsilon^{-1}_{He}(r)\Phi^{M}_{He}(r)} \tag{2}$$

Since no $\bar{He}$ where found over all the measured rigidity range:

$$\int \Phi^{M}_{\bar{He}}(r)dr < 3 \tag{3}$$

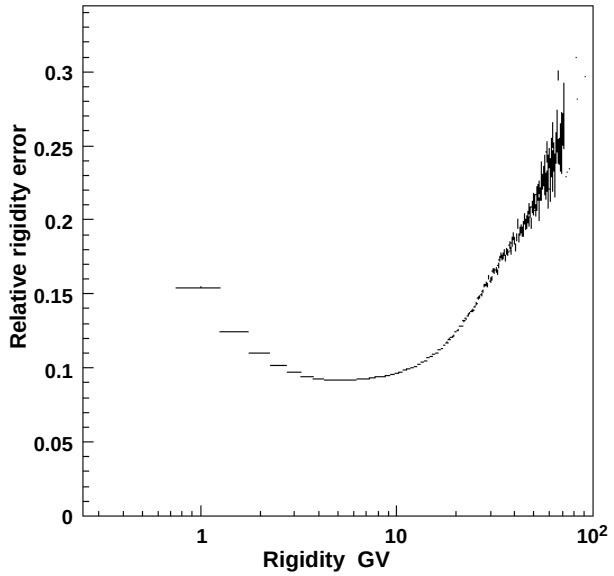

Figure 10: Momentum resolution of the AMS Silicon Tracker for $Z > 1$ particles after having applied the antimatter selection cuts.

With the model dependent assumption that the $\bar{He}$ rigidity spectrum coincide with the He spectrum we obtain:

$$\frac{\Phi_{\bar{He}}}{\Phi_{He}} < 1.14\ 10^{-6} \tag{4}$$

Similarly with $Z > 2$ data we obtain

$$\frac{\Phi_{\bar{Z>2}}}{\Phi_{Z>2}} < 1.9\ 10^{-5} \tag{5}$$

We can also give a conservative upper limit which does not depend on the unknown $\bar{He}$ energy spectrum [19]. We integrate the arguments in equation (2) between r_{min} and r_{max} taking the minimum value of the efficiency in this rigidity interval $\epsilon^{min}_{\bar{He}} = min[\epsilon_{He}(r)]^{r_{max}}_{r_{min}}$. We calculate

$$\frac{\int^{r_{max}}_{r_{min}} \Phi_{\bar{He}} dr}{\int^{r_{max}}_{r_{min}} \Phi_{He} dr} < \frac{3/\epsilon^{min}_{\bar{He}}}{\int^{r_{max}}_{r_{min}} \epsilon^{-1}_{He}(r)\Phi^{M}_{He}(r) dr} \tag{6}$$

which for $r_{min} = 1.6\ GV$ and $r_{max} = 20\ GV$ gives a model independent limit on $\Phi_{\bar{He}}/\Phi_{He}$ of $1.7\ 10^{-6}$ at 95% of CL while for $Z > 2$ the corresponding limit is $2.8\ 10^{-5}$. Figure 11 shows this preliminary result for $\bar{He}$ compared with previous published results [13)– 19)] and the expected AMS sensitivity on the ISS. Our result is better than the best limit published by BESS adding the data of the '93, '94, and '95 flights at 56^o of latitude [19]. It also spans over a larger rigidity interval. For $Z > 2$ our results is about 5 times better than the previous published results [13), 20)]. The large AMS

acceptance made possible to set these stringent limits using only 4 days of exposition to deep space.

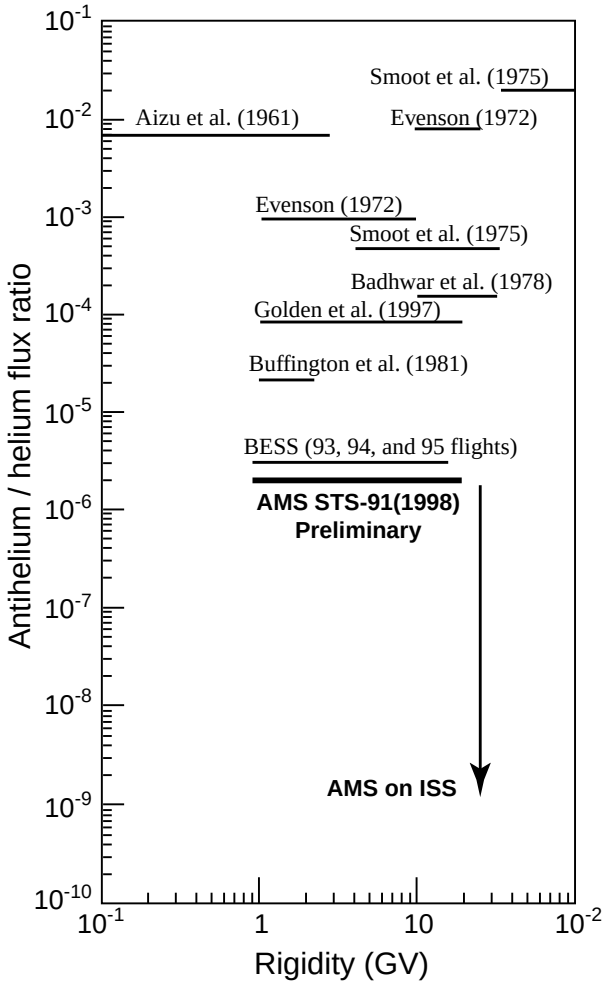

Figure 11: Limits on $\frac{\Phi_{\bar{He}}}{\Phi_{He}}$.

5 Conclusion

The AMS experiment has successfully completed the first precursor flight in June 1998 with an excellent performance of all subsystems, collecting about 100 millions primary CR during 152 orbits around the earth. AMS upper limits on the existence of antimatter improve the results of nearly 40 years of similar searches using stratospheric ballons.

There has never been a sensitive magnetic spectrometer in space covering the energy range up to hundreds of GeV. After its installation on the ISS in 2004, AMS will measure the CR rays composition with an accuracy orders of magnitude

better than before. This instrument will open a new sensitivity window in the search for antimatter and for supersymmetric dark matter in the galactic halo.

References

1 . A.D. Sakharov, *JETP Lett* **5**24 1967.

2 . R.W. Brown and F. Stecker, *Phys. Rev. Lett.* **43**, 315, 1979; K. Sato, PLB **99** 66 1981; A.D. Dolgov, TAC-1996-010 and *astro-ph/9605280*; J.B. Rehm and K. Jedamzik *astro-ph/9802255*; K. Urbanowski WSP-IF 99-55 and *astro-ph/9905279*

3 . K.M. Belotsky *et al.*, MSU-INP 98-31/532 and *astro-ph/9807027*; K.M. Belotsky *et al.*, *astro-ph/9901402*.

4 . G. Steigmann, *Ann. Rev. Astron. Astroph.* **14** 339 1976; E.W. Kolb and M.S. Turner, *Ann. Rev. Nucl. Part. Sci.* **33** 645 1983; P.J.E. Peebles in: *Principles of Physical Cosmology*, (Princeton University Press, Princeton N.J. 1993).

5 . F. Zwickly, *Hel. Phys. Acta* **6** 110 1933.

6 . *Proceedings of DM97* P. Salucci Editor (Studio Editoriale Fiorentino, Firenze Italy 1997).

7 . J. Ellis, J.S. Hagelin, D.V. Nanopulos, K. Olive and M. Srednicki, *Nucl. Phys.* B **238** 453 1984; M.S. Turner and F. Wilzek *Phys. Rev.* D **42** 1001 1990.

8 . B. Chaboyer *et al.*, *Ap. J.* **1** 494 1998.

9 . S.P. Ahlen *et al.*, *Nucl. Instrum. Methods* A**350** 351 1994.

10 . R. Battiston *Nucl. Instrum. Methods (Proc. Suppl.)* B **44** 274 1995; M. Pauluzzi, *Nucl. Instrum. Methods* **A383** 35 1996.

11 . See R. Brun *et al.*, "GEANT 3", CERN DD/EE/84-1 (Revised), September 1987. The GHEISHA program (H. Fesefeldt, RWTH Aachen Report PITHA 85/02 (1985) is used to simulate hadronic interactions.

12 . A.A. Moiseev and J.F. Ormes, *Astropart. Phys.* **6** 379 1997.

13 . G.F. Smoot *et al.*, *Phys. Rev. Lett.* **35** 258 1975.

14 . G. Steigman *et al.*, *Ann. Rev. Astr. Ap.* **14** 339 1976.

15 . G. Badhwar *et al.*, *Nature* **274** 137 1978.

16 . A. Buffington *et al.*, *Ap. J.* **248** 1179 1981.

17 . R.L. Golden *et al.*, *Ap. J.* **479** 992 1997.

18 . J.F. Ormes *et al.*, *Ap. J. Letters* **482** L187 1997.

19 . T. Saeki *et al.*, *Phys. Lett.* **B422** 319 1998.

20 . N. Lund *et al.*, *Astr. and Astroph.* **164** 231 1986.